



Research article

MRI-based radiomic signature as predictive marker for patients with head and neck squamous cell carcinoma

Ying Yuan¹, Jiliang Ren¹, Yiqian Shi, Xiaofeng Tao^{*}

Department of Radiology, Shanghai Ninth People's Hospital, Shanghai Jiao Tong University School of Medicine, Shanghai, China

ARTICLE INFO

Keywords:

Radiomics
 Head and neck squamous cell carcinoma
 Magnetic resonance imaging
 Overall survival
 TNM

ABSTRACT

Purpose: To develop magnetic resonance imaging (MRI)-based radiomic signature and nomogram for preoperatively predicting prognosis in head and neck squamous cell carcinoma (HNSCC) patients.

Method: This retrospective study consisted of a training cohort (n = 85) and a validation cohort (n = 85) of patients with HNSCC. LASSO Cox regression model was used to select the most useful prognostic features with their coefficients, upon which a radiomic signature was generated. The receiver operator characteristics (ROC) analysis and association of the radiomic signature with overall survival (OS) of patients was assessed in both cohorts. A nomogram incorporating the radiomic signature and independent clinical predictors was then constructed. The incremental prognostic value of the radiomic signature was evaluated.

Results: The radiomic signature, consisted of 7 selected features from MR images, was significantly associated with OS of patients with HNSCC ($P < 0.0001$ for training cohort, $P = 0.0013$ for validation cohort). The radiomic signature and TNM stage were proved to be independently associated with OS of HNSCC patients, which therefore were incorporated to generate the radiomic nomogram. In the training cohort, the nomogram showed a better prognostic capability than TNM stage only ($P = 0.005$), which was confirmed in the validation cohort ($P = 0.01$). Furthermore, the calibration curves of the nomogram demonstrated good agreement with actual observation.

Conclusions: MRI-based radiomic signature is an independent prognostic factor for HNSCC patients. Nomogram based on radiomic signature and TNM stage shows promising in non-invasively and preoperatively predicting prognosis of HNSCC patient in clinical practice.

1. Introduction

According to the cancer statistics reported by the National Central Cancer Registry (NCCR) of China, approximately 198,700 new cases of head and neck cancer were diagnosed during 2015, with 63,000 deaths occurring annually [1]. The overall survival (OS) of patient with head and neck squamous cell carcinomas (HNSCC) is relatively low due to high rate of regional and distant metastases at diagnosis. Despite advances in multidisciplinary management, the survival rate of patients with HNSCC has only improved marginally [2,3]. Therefore, new tools are urgently needed to preoperatively identify patients who are at risk of having a poor prognosis, to whom more aggressive treatments should be administered. Tumor stage is traditionally acknowledged to be one

of the most important prognostic factors [4,5]. However, wide spectrum of survival times still exists within the same staged patients.

Medical imaging has the potential to noninvasively assess tumors, and therefore is routinely used in clinical practice for diagnosis and treatment guidance. However, structural based medical images are traditionally evaluated subjectively and qualitatively, partially depending on the readers' experience. The term radiomics has attracted recent interest for providing an easily obtainable opportunity for personalized medicine by extracting quantitative imaging features from conventional medical images, to characterize tumor pathology and heterogeneity [6–9]. Evidence has been accumulating suggesting that radiomics features derived from MRI could bring additional prognostic information in glioblastoma [10–15], nasopharyngeal carcinoma [16],

Abbreviations: 3D, three-dimensional; AJCC, American Joint Committee on Cancer; C-index, concordance index; CT, computed tomography; DICOM, Digital Imaging and Communications in Medicine; HNSCC, head and neck squamous cell carcinomas; LASSO, least absolute shrinkage and selection operator; NCCR, National Central Cancer Registry; OS, overall survival; Rad-score, radiomics score; ROI, region of interests; TE, echo time; TR, repetition time; VOI, volume of interest

^{*} Corresponding author at: Department of Radiology, Shanghai Ninth People's Hospital, Shanghai Jiao Tong University School of Medicine, 639 Zhizaoju Road, 200011 Shanghai, China.

E-mail address: cjr.taoxiaofeng@vip.163.com (X. Tao).

¹ These authors contributed equally to this work.

<https://doi.org/10.1016/j.ejrad.2019.06.019>

Received 15 February 2019; Received in revised form 18 June 2019; Accepted 23 June 2019

0720-048X/© 2019 Elsevier B.V. All rights reserved.

prostate cancer [17] and renal cell cancer [18], and serve as prognostic biomarkers.

In prognostic studies of patients with HNSCC, computed tomography (CT)-based radiomics has been demonstrated to be valuable [19–21]. Compared to CT, head and neck MRI has potential advantage of better soft tissue contrast and less artifact [22], which could be expected to bring more information. However, the ability of MRI-based radiomic features for predicting prognosis in HNSCC patients has not been evaluated yet. Therefore, the aim of the current study was to determine whether radiomic features derived from MRI could help to predict the prognosis of HNSCC patients and improve prognostic ability by combining with clinical factors.

2. Materials and methods

2.1. Patient selection and clinical follow-up

This retrospective study was approved by Institutional Review Board, and the requirement of informed consent was waived. Patients with histopathologically confirmed HNSCC, who underwent preoperative MRI and received treatment in our institution from January 2013 to December 2015, were collected. Patients were excluded for any of the following reasons: (1) tumor size smaller than 5 mm; (2) imaging artifacts (motion or susceptibility artifacts) impaired correct segmentation; (3) had any prior history of head and neck cancer; or (4) received treatment (surgery or chemoradiation) for the cancer before MR scan.

Clinical characteristics were collected from the medical records, including gender, age, smoking status, alcohol use, TNM stage, and treatments. Tumor stage was decided on the American Joint Committee on Cancer (AJCC) TNM Staging Manual [23]. Patients were defined as “ever smokers,” if they smoked at least 100 cigarettes during their lifetime, and “never smokers” otherwise. “Ever drinkers” were defined as those who drunk at least one alcoholic beverage per week for at least one year, and as “never drinkers” otherwise [24]. The follow-up endpoint of the study was OS. OS time was defined as the time interval from the date of preoperative MRI scan until the date of death from any cause or the last follow-up date (March 31, 2017).

2.2. MRI acquisition and segmentation

MRI examinations were performed on a 1.5-T scanner (Signa Excite; GE Medical Systems, Milwaukee, Wisconsin, USA). The imaging protocol included axial T1-weighted (T1W) imaging (repetition time [TR]/echo time [TE], 400–600/10 ms), axial T2W imaging (TR/TE, 3200/100 ms). Other parameters were matrix, 256 × 192 mm; field of view, 240 × 240 mm, and thickness/gap, 5/1 mm. The T1W images were not used for further study since the margin of HNSCC could not be clearly identified, which impaired correct segmentation.

For feature selection, we chose axial T2W Digital Imaging and Communications in Medicine (DICOM) images archived in the PACS (Centricity Radiology RA600, GE Healthcare). ITK-SNAP software (open source software; www.itk-snap.org) was adopted for manual segmentation. Manual segmentation of the cancer was firstly performed by two radiologists (Y.Y. and J.R.; with head and neck MRI interpretation experience of 15 years and 10 years respectively). They worked together by consensus under supervision of a senior radiologist (X.T.) with 25 years of experience. The reviewers were all blinded to results from other imaging modalities, histopathologic reports and follow-up data. By stacking up region of interests (ROIs) delineated slice-by-slice on T2W images, the three-dimensional (3D) volume of interest (VOI) covered the whole tumor was acquired.

2.3. Data analysis

All included patients were randomly divided into training cohort

and validation cohort at a ratio of 1:1 using computer-generated random numbers. The clinical characteristics of gender, age, smoking status, alcohol using, TNM stage, treatments and OS time were compared between the training and validation cohorts by the independent samples *t* test, χ^2 test, or Mann-Whitney U test, where appropriate.

2.3.1. Radiomics signature building

Totally 485 radiomic features were extracted from T2W images of each patient, which described the first-order intensity statistics, texture features, and shape and size of the 3D tumor region. First-order intensity statistics and textural features were recomputed after different wavelet decomposition in three directions (x, y, z) of the original images. All feature extraction methods were implemented using MatLab 2014a (MathWorks, Natick, MA, USA). The details of feature extraction and selection methods were described previously [16]. We used least absolute shrinkage and selection operator (LASSO) Cox regression model to select features most significant in the training cohort. After using LASSO Cox regression models, features with non-zero coefficient were finally selected. Then a radiomic signature was built through a linear combination of selected features weighted by their coefficients generated from LASSO Cox regression models. A radiomics score (Rad-score) was calculated for each patient upon the radiomic signature.

2.3.2. Validation of radiomic signature

The association of the radiomic signature with OS of HNSCC patients was assessed in the training cohort with univariate Cox analysis, and validated in the validation cohort. We assessed the prognostic accuracy of the radiomic signature in the training and validation cohorts using receiver operator characteristics (ROC) analysis. The patients were classified into high-risk or low-risk groups according to the cut point defined from ROC curve in training cohort. The Kaplan-Meier survival curves of the high-risk and low-risk groups was compared using a weighted log-rank test (the G-rho rank test, $\rho = 1$). Furthermore, multivariable Cox proportional hazards model (backward step-down selection; the Akaike information criterion) was adopted to test the prognostic ability of radiomic signature, gender, age, smoking, alcohol using, TNM stage, and treatments.

2.3.3. Assessment of radiomic nomogram

By incorporating significant predictors from multivariable Cox proportional hazards model, a nomogram was generated. The prognostic performance of the nomogram, as well as radiomic signature, was measured using the concordance indexes (C-indexes) and compared between models in both the training and validation cohorts. The validation data was only used to test the model and not to alter the model in any way. The value of the C-index can range from 0.5, which shows no discriminative ability, to 1.0, which indicates perfect ability to distinguish the patients who experience death and those who do not. Calibration curves were also generated to evaluate the agreement between actual observations with nomogram prediction, by plotting the observed actual survival fraction against the nomogram-assessed probabilities.

2.3.4. Statistical analysis

The statistical analyses were performed with R software (R Core Team. R: A language and environment for statistical computing. R Foundation for Statistical Computing, Vienna, Austria. URL: <http://www.R-project.org>, 2016). The following R packages were used. The glmnet package was used for LASSO logistic regression. The rms package was used for Cox proportional hazards regression, nomograms, and calibration curves. The Hmisc package was used for comparisons between C-indexes. All statistical analyses were two sided, with the statistical significance level set at 0.05.

Table 1
Demographic and clinical characteristics of patients with HNSCC.

Characteristics	Training cohort N (%)	Validation cohort N (%)	P value
Gender			0.49
Male	63 (74.1%)	58 (68.2%)	
Female	22 (25.9%)	27 (31.8%)	
Age			0.16
Median ^a	58 (50–63)	60 (53–66)	
< 60	53 (62.4%)	44 (51.8%)	
≥ 60	32 (37.6%)	41 (48.2%)	
Smoking			0.17
Yes	36 (42.4%)	27 (31.8%)	
No	49 (57.6%)	58 (68.2%)	
Alcohol use			0.22
Yes	26 (30.6%)	18 (21.2%)	
No	59 (69.4%)	67 (78.8%)	
Treatment			
S + /-C/X	66 (77.6%)	60 (70.6%)	
C/X	14 (16.5%)	18 (21.2%)	
Other	5 (5.9%)	7 (8.2%)	
TNM stage			0.25
I-II	25 (29.4%)	33 (38.8%)	
III-IV	60 (70.6%)	52 (61.2%)	
T stage			0.62
T1	16 (18.8%)	19 (22.4%)	
T2	40 (47.1%)	43 (50.6%)	
T3	7 (8.2%)	7 (8.2%)	
T4	22 (25.9%)	16 (18.8%)	
N stage			0.09
N0	35 (41.2%)	39 (45.9%)	
N1	27 (31.8%)	15 (17.6%)	
N2	23 (27.0%)	31 (36.5%)	
Follow-up time (day)			
Median ^a	1024 (626–1145)	1014 (585–1184)	
Rad-score			0.48
Median ^a	6.01 (5.58–6.47)	5.90 (5.24–6.55)	

C = chemotherapy, S = surgery, X = radiotherapy.

^a Data in parentheses is interquartile range.

3. Results

3.1. Clinical characteristics and OS

A total of 170 patients were included (121 male, 49 female; mean age 59.0 ± 22.9 years). Respectively 85 and 85 patients were randomly allocated into the training cohort and the validation cohort. The clinical characteristics of the patients are summarized in Table 1. No statistical difference was found between the two cohorts in terms of clinical characteristics and follow-up data (all $P > 0.05$). The median OS time was 1019 days for all patients (range, 52–1599 days). During the follow-up period, 60 patients (35.3%) had experienced a confirmed death.

3.2. Radiomic signature building

Radiomics workflow is illustrated in Fig. 1, including segmentation, feature extraction, and predictive model building. Among the 485 features extracted from T2W images, 53 features were significantly associated with OS of HNSCC patients in univariate Cox analysis. After using LASSO Cox regression models, 7 features with non-zero coefficient were finally selected (Fig. 2). Thereafter, the radiomic signature was constructed upon the 7 features and their coefficients. Rad-score was calculated for each patient with the following formula:

$$\text{Rad - score} = -0.2314517 \times X0_{\text{fos_entropy_p-13.1217}} \times X0_{\text{fos_uniformity_p-8.5746}} \times X3_{\text{fos_skewness}} + 0.0238 \times X4_{\text{fos_maximum}} + 0.1890 \times X3_{\text{GLCM_variance}} + 7.3992 \times X7_{\text{GLCM_correlation}} + 0.1119 \times X1_{\text{GLRLM_mean}}$$

3.3. Validation of radiomic signature

The Rad-score in training and validation cohorts showed no significant difference ($P = 0.48$; see Table 1). In the training cohort, the radiomic signature was significantly associated with OS of HNSCC patients ($P < 0.0001$; HR = 3.83, 95% confidence interval [CI]: 2.28–6.44), which was confirmed in the validation cohort ($P = 0.0013$; HR = 1.84; 95% CI: 1.35–2.51). The area under the ROC curve (AUC) was calculated to evaluate the prognostic accuracy of the radiomic signature. The AUC values were 0.78 and 0.76 for the training and validation cohorts, respectively (Fig. 3). Based on the cutoff value (Rad-score 5.85) generated from ROC for the training cohort, the patients were classified into high-risk group (Rad-score > 5.85) and low-risk group (Rad-score ≤ 5.85) in the training and validation cohort, respectively. Log-rank test verified that the patients in the low-risk group experienced better survival than the patients in the high-risk group in the training cohort ($P < 0.001$), as well as in the validation cohort ($P = 0.007$) (Fig. 4). The multivariable Cox proportional hazards model found that radiomic signature and tumor stage were significant predictors in HNSCC patients (radiomic signature: HR: 3.25, 95% CI: 1.90–5.55, $P < 0.001$; stage: HR: 3.41, 95% CI: 1.01–2.35, $P = 0.048$), while gender, age, smoking status, alcohol use and treatment were not (all $P > 0.05$).

3.4. Incremental value of radiomic signature in OS prediction

The nomogram was generated combining radiomic signature and TNM stage (Fig. 5). To demonstrate the incremental prognostic value of the radiomic signature to the traditional TNM staging system, C-indexes were calculated and compared. C-indexes for the different models, including the radiomic signature, TNM stage and nomogram, and the comparative results are listed in Table 2. In the training cohort, the radiomic nomogram showed a better prognostic capability (C-index: 0.76; 95% CI: 0.66–0.87) than TNM stage (C-index: 0.63; 95% CI: 0.55–0.72; $P = 0.005$ for comparison). In the validation cohort, a better prognostic ability was also observed in radiomic nomogram (C-index: 0.72; 95% CI: 0.63–0.82) than stage (C-index: 0.61; 95% CI: 0.51–0.71; $P = 0.01$ for comparison). Furthermore, the C-indexes of radiomic signature were also significantly higher than those of the TNM stage both in the training cohort ($P = 0.027$) and validation cohort ($P = 0.035$). The calibration curves of the nomograms for the probability of death at 1-, 2- and 3- years are shown in Fig. 6, demonstrating good agreement between actual observation and the estimation upon the radiomic nomogram.

4. Discussion

The term radiomics has attracted increased attention in recent years for enabling a noninvasive, low cost and repeatable way to extract quantitative features from conventional medical images, and potentially contributing as decision support for personalized medicine. In the current study, we extracted 485 radiomic features quantifying intensity, shape and texture from pretreatment T2W images of patients with HNSCC. In the HNSCC patients, we selected radiomic features with the highest prognostic power and built a 7-feature based radiomic signature, which was validated as a significant OS predictor for patients with HNSCC. Compared with TNM stage, the radiomic signature showed significantly better prognostic performance. The nomogram, combining TNM stage and radiomic signature, outperformed TNM stage, and serve as potential prognostic marker of HNSCC patients.

Previously, the predictive value of CT-based radiomics in HNSCC patients has been investigated by extracting 440 radiomic features from pretreatment CT images [20,21]. For feature selection, consensus clustering method was adopted [20], or the single best performing radiomic feature was selected from each of the four feature groups including ‘Statistics Energy’, ‘Shape Compactness’, ‘Grey Level

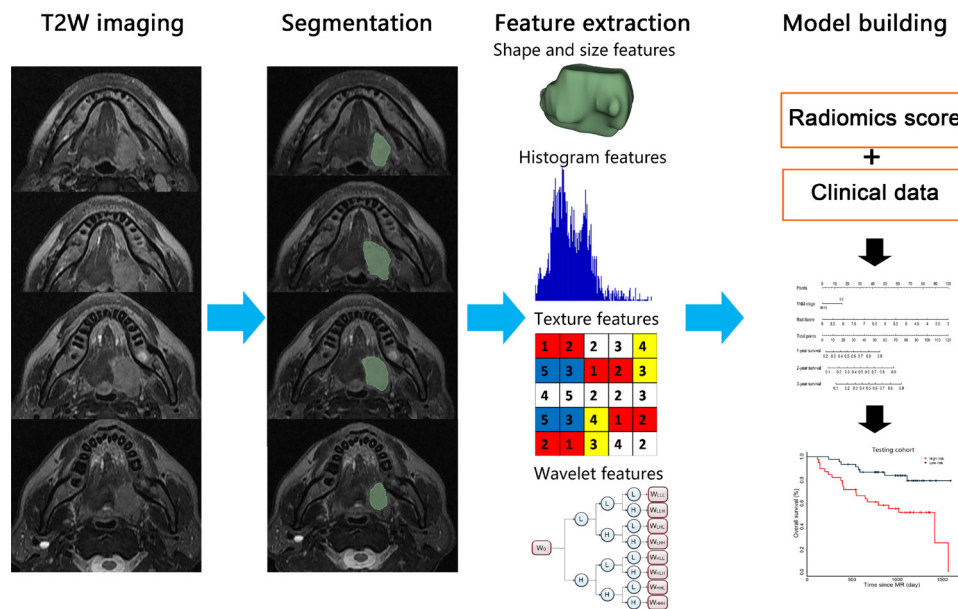


Fig. 1. Flowchart shows the process of radiomics.

Nonuniformity’ and ‘Grey Level Nonuniformity HLH’ [21]. Despite of diversity in feature selection procedure, the prognostic performance of CT based radiomic signature in both studies was confirmed. In the current study, LASSO Cox regression model was used for feature selection, which is suitable for the regression of high-dimensional data [25] and is employed in recent radiomic studies more than once [16,26,27]. The LASSO method is an estimation technique in which the estimated regression coefficients are constrained toward zero. Variable selection is achieved by choosing the remaining nonzero coefficients to reflect the overfitting caused by data-based model selection.

For the better soft tissue contrast and correspondingly more comprehensive texture information anticipated in MR images than CT, we evaluate the predictive value of MRI-based radiomic signature in HNSCC patients. The C-indexes of radiomic signature in the current study were 0.73 in the training cohort and 0.71 in the validation cohort, which were higher than those reported in previous CT-based radiomic studies (C-index 0.68–0.69) [20,21]. One recently published study compared the ability of CT- and MRI-based radiomic features to differentiate benign from malignant pleural lesions [28]. The CT model with best discriminative ability showed an AUC of 0.92, while the most discriminative MRI model showed a slightly lower performance with AUC of 0.87. The superior performance of CT could be attributed to the finer spatial resolution and less evident motion artifact to facilitate the segmentation of pleural lesions from adjacent structures. However, in

head and neck MRI, motion artifact is less evident than chest MRI, and superior performance still could be expected for MRI. Further studies are warranted to compare the predictive value of CT and MRI-based radiomic signature in same cohort of HNSCC patients.

Incorporating the radiomic signature with clinical risk factors into an easy-to-use nomogram facilitates the clinical application. In the current study, we developed and validated a nomogram, incorporating the radiomic signature and TNM stage, for preoperative prediction of OS in patients with HNSCC. The TNM staging system is extensively used for risk stratification and treatment decision making. Both T and N classification are independent prognostic factor for patients with locally advanced HNSCC [5]. However, wide spectrum of survival times still exists within the same staged patients. In the current study, the C-indexes of radiomic signature and nomogram were significantly higher than that of the TNM stage, indicating a better performance in discriminating high-risk patients using radiomic signature or nomogram. Both in the training cohort and validation cohort, the radiomic nomogram showed a better predicting capability than that of the TNM stage alone, with the C-index of nomogram as high as 0.76. In the previous study evaluating CT-based radiomics for predicting OS of HNSCC patients [21], a significant improvement was also demonstrated after incorporating the radiomic signature with TNM staging, compared with using TNM stage alone. In another study of advanced nasopharyngeal carcinoma (NPC), the predictive value of MRI-based radiomics was also

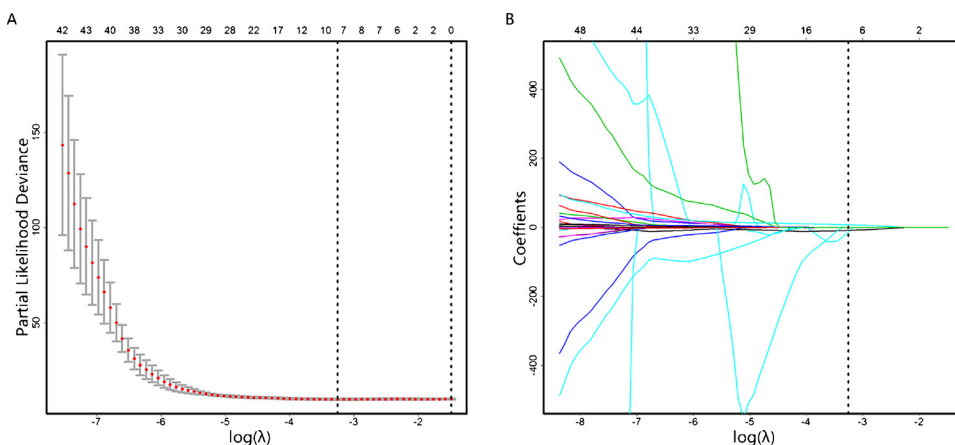


Fig. 2. Feature selection using the least absolute shrinkage and selection operator (LASSO) Cox model. (A) Tuning parameter (λ) selection in the LASSO Cox model used 10-fold cross-validation with minimum criteria. The partial likelihood deviance was plotted versus $\log(\lambda)$. Dotted vertical lines were drawn at the optimal values by using the minimum criteria and the standard error of the minimum criteria. (B) LASSO coefficient profiles of the 53 radiomics features. A coefficient profile was plotted against the $\log(\lambda)$ sequence. Vertical line was drawn at the value selected using 10-fold cross-validation, where optimal λ resulted in 7 non-zero coefficients.

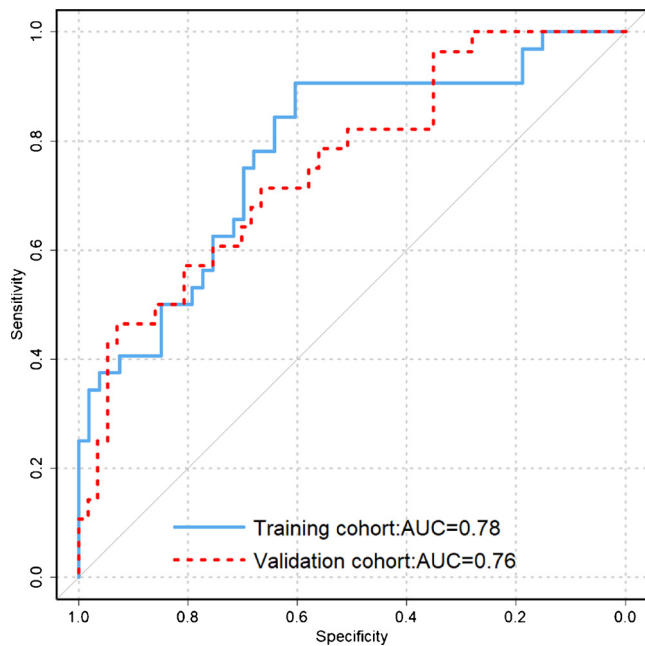


Fig. 3. ROC curves for radiomic signature in training cohort and validation cohort.

evaluated using radiomic signature and nomogram [16]. In the current study, we focused on different tumor entities of HNSCC, which mostly were oral cavity and oropharyngeal SCC, though a similar predictive power was acquired with a C-index of radiomics nomogram of 0.76 in the current study, which was 0.77 in the NPC study.

The current study reveals significant prognostic potential of T2W MRI based radiomic signature and radiomic nomogram, however it has some limitations. First, besides the clinical risk factors we assessed in the current study, human papilloma virus (HPV) infection is one prominent risk factor of HNSCC, especially for oral SCC. Infection with high-risk types of the HPV is an etiological risk factor for HNSCC and associated with a better response to therapy and improved survival. However, we fail to collect HPV16 validation results from patients since we did not routinely do serology validation for HPV16 in HNSCC patients in our hospital. The incidence rate of HPV infectious in Chinese population is apparently lower compared to the western. In a multicenter case-control study conducted in southern Chinese population, high-risk HPV infection was only found in 7.5% of HNSCC patients, and only 5.3% samples had evidence of viral integration [29], significantly lower than in western countries [30]. Nevertheless, on account of the significance of HPV infection in pathogenesis and prognosis of HNSCC, our findings need to be confirmed in other cohorts with known HPV status in the future. Secondly, we retrospectively included a single team with an internal validation. The reproducibility of our model under

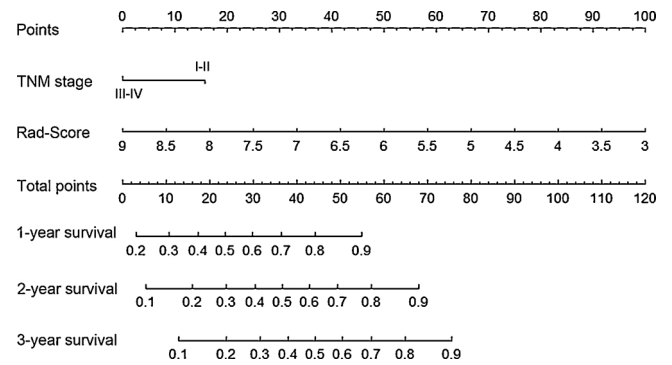


Fig. 5. Radiomics nomogram. Locate the patient’s Rad-score on the Rad-score axis. Draw a line straight upward to the Points’ axis to determine how many points toward the probability of OS the patient receives for the Rad-score. Repeat the process for TNM stage. Sum the points achieved for radiomic signature and stage. Locate the sum on the Total Point axis. Draw a line straight down to find the patient’s probability of 1-, 2- and 3-year OS.

Table 2

Prognostic performance of radiomic signature, AJCC staging system and radiomic nomogram.

Model	Training cohort			Validation cohort		
	C-index	95% CI	P value	C-index	95% CI	P value
Radiomics signature	0.73	0.63~0.84	0.027 ^a	0.71	0.59~0.82	0.035 ^a
AJCC staging system	0.63	0.55~0.72	0.005 ^b	0.61	0.51~0.71	0.01 ^b
Radiomics nomogram	0.76	0.66~0.87	0.256 ^c	0.72	0.63~0.82	0.369 ^c

^a P value of comparison between C-index of radiomic signature and the AJCC staging system.

^b P value of comparison between C-index of AJCC staging system and the radiomic nomogram.

^c P value of comparison between C-index of radiomic signature and radiomic nomogram.

different imaging settings should be justified via more external validation in the future. A large-scale prospective multicenter validation cohort is warranted to assess the generalizability of the reported findings.

5. Conclusions

The current study developed and validated pretreatment T2W-MRI based radiomics as a convenient approach to predict OS in patients with HNSCC. The radiomic signature complements traditional staging system in the radiomic nomogram, which potentially serves as decision

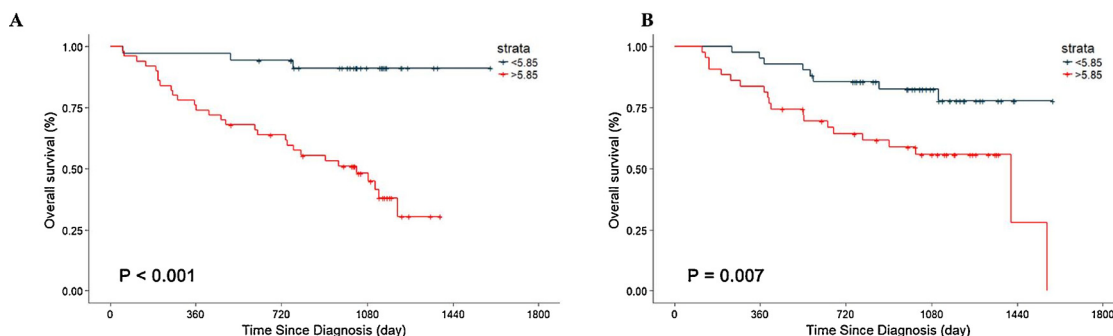


Fig. 4. Kaplan-Meier survival analyses of patients in the training and validation cohort. A significant association of the radiomic signature with OS of patients was shown in the training cohort (A), which was validated in the validation cohort (B).

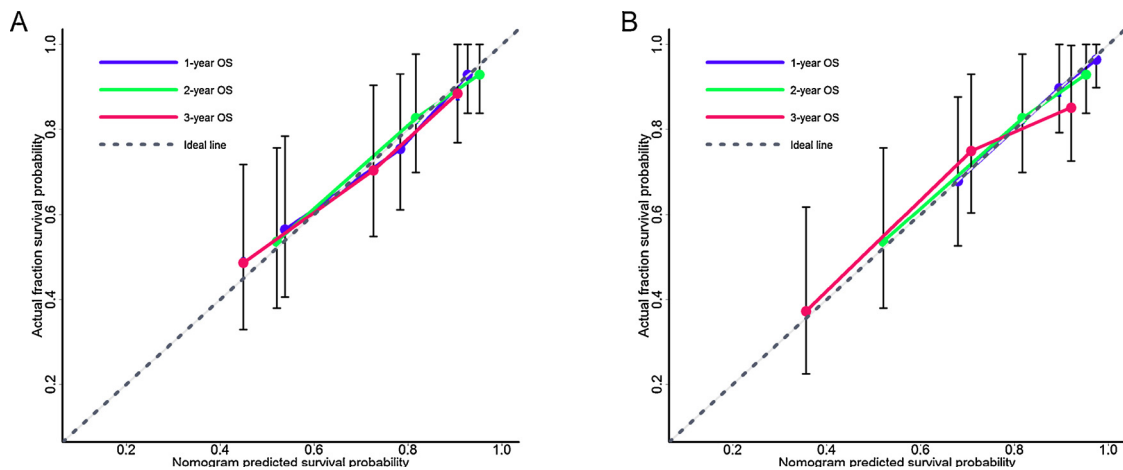


Fig. 6. Calibration curves of the radiomic nomogram. The curves show good agreement between the predicted and the actual 1-, 2- and 3-year OS in the training cohort (A) and validation cohort (B). Nomogram predicted OS probability is plotted on the x-axis; the actual OS rate is plotted on the y-axis. Diagonal dotted line: a perfect estimation by an ideal model, in which the estimated outcome perfectly corresponds to the actual outcome. Solid line: performance of the radiomic nomogram, a closer lining of which with the diagonal dotted line represents a better estimation.

support for personalized medicine. The current study provides an inspiring attempt for non-invasive pretreatment evaluation of HNSCC, which may help directing individual treatment strategies for patients with HNSCC in the future.

Disclosure paragraph

The authors of this manuscript declare no relationships with any companies, whose products or services may be related to the subject matter of the article.

Sources of support

This work was supported by funds from the National Scientific Foundation of China (91859202, 81771901), and Clinical Research Plan of SHDC (SHDC22015023).

References

- [1] W. Chen, R. Zheng, P.D. Baade, S. Zhang, H. Zeng, F. Bray, et al., Cancer statistics in China, 2015, *CA Cancer J. Clin.* 66 (2) (2016) 115–132.
- [2] R.L. Siegel, K.D. Miller, A. Jemal, Cancer Statistics, 2017, *CA Cancer J. Clin.* 67 (2017) 7–30.
- [3] L.A. Torre, F. Bray, R.L. Siegel, J. Ferlay, J. Lortet-Tieulent, A. Jemal, Global cancer statistics, 2012, *CA Cancer J. Clin.* 65 (2015) 87–108.
- [4] J. Ju, J. Wang, C. Ma, Y. Li, Z. Zhao, T. Gao, et al., Nomograms predicting long-term overall survival and cancer-specific survival in head and neck squamous cell carcinoma patients, *Oncotarget* 7 (2016) 51059–51068.
- [5] Y. Xing, J. Zhang, H. Lin, K.A. Gold, E.M. Sturgis, A.S. Garden, et al., Relation between the level of lymph node metastasis and survival in locally advanced head and neck squamous cell carcinoma, *Cancer* 122 (2016) 534–545.
- [6] E. Sala, E. Mema, Y. Himoto, H. Veeraraghavan, J.D. Brenton, A. Snyder, et al., Unravelling tumour heterogeneity using next-generation imaging: radiomics, radiogenomics, and habitat imaging, *Clin. Radiol.* 72 (2017) 3–10.
- [7] R.T. Larue, G. Defraene, D. De Ruysscher, P. Lambin, W. van Elmpt, Quantitative radiomics studies for tissue characterization: a review of technology and methodological procedures, *Br. J. Radiol.* 90 (2017) 20160665.
- [8] P. Lambin, E. Rios-Velazquez, R. Leijenaar, S. Carvalho, R.G. van Stiphout, P. Granton, et al., Radiomics: extracting more information from medical images using advanced feature analysis, *Eur. J. Cancer* 48 (2012) 441–446.
- [9] V. Kumar, Y. Gu, S. Basu, A. Berglund, S.A. Eschrich, M.B. Schabath, et al., Radiomics: the process and the challenges, *Magn. Reson. Imaging* 30 (2012) 1234–1248.
- [10] S.D. McGarry, S.L. Hurrell, A.L. Kaczmarowski, E.J. Cochran, J. Connelly, S.D. Rand, et al., Magnetic resonance imaging-based radiomic profiles predict patient prognosis in newly diagnosed glioblastoma before therapy, *Tomography* 2 (2016) 223–228.
- [11] Y. Cui, S. Ren, K.K. Tha, J. Wu, H. Shirato, R. Li, Volume of high-risk intratumoral subregions at multi-parametric MR imaging predicts overall survival and complements molecular analysis of glioblastoma, *Eur. Radiol.* 27 (9) (2017) 3583–3592.
- [12] P. Kickingereder, M. Götz, J. Muschelli, A. Wick, U. Neuberger, R.T. Shinohara,

- et al., Large-scale radiomic profiling of recurrent glioblastoma identifies an imaging predictor for stratifying anti-angiogenic treatment response, *Clin. Cancer Res.* 22 (2016) 5765–5771.
- [13] P. Prasanna, J. Patel, S. Partovi, A. Madabhushi, P. Tiwari, Radiomic features from the peritumoral brain parenchyma on treatment-naïve multi-parametric MR imaging predict long versus short-term survival in glioblastoma multiforme: Preliminary findings, *Eur. Radiol.* 27 (10) (2017) 4188–4197.
- [14] P.O. Zinn, S.K. Singh, A. Kotrotsou, F. Zandi, G. Thomas, M. Hatami, et al., Clinically applicable and biologically validated MRI radiomic test method predicts glioblastoma genomic landscape and survival, *Neurosurgery* 63 (Suppl 1) (2016) 156–157.
- [15] A. Rao, G. Rao, D.A. Gutman, A.E. Flanders, S.N. Hwang, D.L. Rubin, et al., A combinatorial radiographic phenotype may stratify patient survival and be associated with invasion and proliferation characteristics in glioblastoma, *J. Neurosurg.* 124 (2016) 1008–1017.
- [16] B. Zhang, J. Tian, D. Dong, D. Gu, Y. Dong, L. Zhang, et al., Radiomics features of multiparametric MRI as novel prognostic factors in advanced nasopharyngeal carcinoma, *Clin. Cancer Res.* 23 (15) (2017) 4259–4269.
- [17] K. Gnep, A. Fargeas, R.E. Gutiérrez-Carvajal, F. Commandeur, R. Mathieu, J.D. Ospina, et al., Haralick textural features on T2-weighted MRI are associated with biochemical recurrence following radiotherapy for peripheral zone prostate cancer, *J. Magn. Reson. Imaging* 45 (2017) 103–117.
- [18] N. Jamshidi, E. Jonasch, M. Zapala, R.L. Korn, J.D. Brooks, B. Ljungberg, M.D. Kuo, The radiogenomic risk score stratifies outcomes in a renal cell cancer phase 2 clinical trial, *Eur. Radiol.* 26 (2016) 2798–2807.
- [19] C. Parmar, P. Grossmann, D. Rietveld, M.M. Rietbergen, P. Lambin, H.J. Aerts, Radiomic machine-learning classifiers for prognostic biomarkers of head and neck Cancer, *Front. Oncol.* 5 (2015) 272.
- [20] C. Parmar, R.T. Leijenaar, P. Grossmann, E. Rios Velazquez, J. Bussink, D. Rietveld, et al., Radiomic feature clusters and prognostic signatures specific for Lung and Head & Neck cancer, *Sci. Rep.* 5 (2015) 11044.
- [21] H.J. Aerts, E.R. Velazquez, R.T. Leijenaar, C. Parmar, P. Grossmann, S. Carvalho, et al., Decoding tumour phenotype by noninvasive imaging using a quantitative radiomics approach, *Nat. Commun.* 5 (2014) 4006.
- [22] D.W. Tshering Vogel, H.C. Thoeny, Cross-sectional imaging in cancers of the head and neck: how we review and report, *Cancer Imaging* 16 (1) (2016) 20.
- [23] S.H. Huang, B. O'Sullivan, Overview of the 8th edition TNM classification for head and neck cancer, *Curr. Treat. Options Oncol.* 18 (7) (2017) 40.
- [24] C. Zhang, E.M. Sturgis, H. Zheng, X. Song, P. Wei, L. Jin, et al., Genetic variants in TNF- α promoter are predictors of recurrence in patients with squamous cell carcinoma of oropharynx after definitive radiotherapy, *Int. J. Cancer* 134 (2014) 1907–1915.
- [25] R. Tibshirani, The lasso method for variable selection in the Cox model, *Stat. Med.* 16 (4) (1997) 385–395.
- [26] Y.Q. Huang, C.H. Liang, L. He, J. Tian, C.S. Liang, X. Chen, et al., Development and validation of a radiomics nomogram for preoperative prediction of lymph node metastasis in colorectal Cancer, *J. Clin. Oncol.* 34 (2016) 2157–2164.
- [27] Y. Huang, Z. Liu, L. He, X. Chen, D. Pan, Z. Ma, et al., Radiomics signature: a potential biomarker for the prediction of disease-free survival in early-stage (I or II) non-small cell lung Cancer, *Radiology* 281 (2016) 947–957.
- [28] E. Pena, M. Ojiaku, J.R. Inacio, A. Gupta, D.B. Macdonald, W. Shabana, et al., Can CT and MR Shape and textural features differentiate benign versus malignant pleural lesions? *Acad. Radiol.* (2017) pii: S1076-6332(17)30133-2.
- [29] J.S. Chor, A.C. Vlantis, T.L. Chow, S.C. Fung, F.Y. Ng, C.H. Lau, et al., The role of human papillomavirus in head and neck squamous cell carcinoma: a case control study on a southern Chinese population, *J. Med. Virol.* 88 (2016) 877–887.
- [30] A. Zaravinos, An updated overview of HPV-associated head and neck carcinomas, *Oncotarget* 5 (2014) 3956–3969.